Title
Assessing the impacts of different WRF precipitation physics in hurricane simulations

Journal
Weather and Forecasting, 27(4)

ISSN
0882-8156

Authors
Nasrollahi, N
Aghakouchak, A
Li, J
et al.

Publication Date
2012

DOI
10.1175/WAF-D-10-05000.1

Assessing the Impacts of Different WRF Precipitation Physics in Hurricane Simulations

NASRIN NASROLLAHI, AMIR AGHAKOUCHAK, JIALUN LI, XIAOGANG GAO, KUOLIN HSU, AND SOROOSH SOROOSHIAN

Center for Hydrometeorology and Remote Sensing, University of California, Irvine, Irvine, California

(Manuscript received 14 July 2010, in final form 23 February 2012)

ABSTRACT

Numerical weather prediction models play a major role in weather forecasting, especially in cases of extreme events. The Weather Research and Forecasting Model (WRF), among others, is extensively used for both research and practical applications. Previous studies have highlighted the sensitivity of this model to microphysics and cumulus schemes. This study investigated the performance of the WRF in forecasting precipitation, hurricane track, and landfall time using various microphysics and cumulus schemes. A total of 20 combinations of microphysics and cumulus schemes were used, and the model outputs were validated against ground-based observations. While the choice of microphysics and cumulus schemes can significantly impact model output, it is not the case that any single combination can be considered ''ideal'' for modeling all characteristics of a hurricane, including precipitation amount, areal extent, hurricane track, and the time of landfall. For example, the model's ability to simulate precipitation (with the least total bias) is best achieved using Betts–Miller–Janjić (BMJ) cumulus parameterization in combination with the WRF single-moment five-class microphysics scheme (WSM5). It was determined that the WSM5–BMJ, WSM3 (the three-class version of the WSM scheme)–BMJ, and Ferrier microphysics in combination with the Grell–Devenyi cumulus scheme were the best combinations for simulation of the landfall time. However, the hurricane track was best estimated using the Lin et al. and Kessler microphysics options with BMJ cumulus parameterization. Contrary to previous studies, these results indicated that the use of cumulus schemes improves model outputs when the grid size is smaller than 10 km. However, it was found that many of the differences between parameterization schemes may be well within the uncertainty of the measurements.

1. Introduction

Atmospheric phenomena have profound impacts on our economy and lives. Hurricanes are one of the most severe and threatening weather events to humans, and can cause major damage to the eastern and southeastern United States each year. They may result in extreme precipitation and subsequent flooding events, both of which pose a significant concern to the population and exert a major negative impact on economic growth. Reliable prediction of atmospheric variables (e.g., precipitation, wind direction, and velocity) can play a significant role in reducing the vulnerability of our society to severe events. However, the prediction of precipitation structure is extremely challenging.

Based on initial conditions, regional weather models currently estimate the state of the near-future atmosphere by solving atmosphere dynamic and thermodynamic equations. Some weather models include different physics options that describe the physical processes of the atmospheric phenomena. Two of the most important physics options are the microphysics and cumulus parameterizations. The microphysics option provides atmospheric heat and moisture tendencies. It also accounts for the vertical flux of precipitation and the sedimentation process (Skamarock et al. 2007). Unlike the microphysics option, the cumulus parameterization is used to vertically redistribute heat and moisture independent of latent heating due to precipitation.

The Weather Research and Forecasting model (WRF) is a mesoscale modeling system designed to improve the weather forecasts. The WRF has different physical

Corresponding author address: Nasrin Nasrollahi, Center for Hydrometeorology and Remote Sensing, Dept. of Civil and Environmental Engineering, University of California, Irvine, Irvine, CA 92617.
E-mail: nasrin.n@uci.edu

DOI: 10.1175/WAF-D-10-05000.1

(i.e., microphysical and cumulus) parameterization schemes that influence how the state of the system changes with time. Choosing the right model physical parameterization can help us predict weather variables more accurately.

Previous studies (e.g., Fovell 2006) demonstrated that different model options may result in significant variability in the predictions. In a recent study, Fovell et al. (2010) showed that numerical weather prediction models are particularly sensitive to the interaction of various microphysics and radiation schemes. Their study revealed that the model's sensitivity to microphysics is significantly less when cloud radiative feedback is not utilized. Additionally, work done by Lowrey and Yang (2008) investigated major precipitation errors that arose from physical and cumulus parameterizations, the buffer zone, the initialization interval, the domain size, and the initial and boundary conditions. The authors concluded that precipitation is actually more sensitive to cumulus schemes than to cloud microphysics options. Following this, Jankov et al. (2007) examined various combinations of cumulus convection schemes, microphysical options, and boundary conditions. Their results showed that no configuration was significantly better at all times. Furthermore, the variability of predictions was more significant with respect to the choice of the cumulus option. However, to a lesser extent, the choice of microphysical scheme affected the variability of the predictions. Gallus (1999) and Wang and Seaman (1997) also confirmed the influence of cumulus schemes in simulations of precipitation patterns. While the microphysical options and cumulus schemes have been widely explored in the literature, it is important to remember this does not discount the fact that there are other physical parameters and model configuration settings that can affect the WRF predictions (e.g., atmospheric radiation, planetary boundary layer, lateral boundary condition, domain size).

Warm season convective storms are the most difficult storms to model with numerical weather prediction models (Olson et al. 1995; Zhang et al. 2006; Lowrey and Yang 2008). The importance of capturing the space–time variability of precipitation, as well as its impacts on the quality of runoff predictions, is emphasized in many previous studies (Fiener and Auerswald 2009; Corradini and Singh 1985; Goodrich et al. 1995; Arnaud et al. 2002). The significance of microphysics and cumulus parameterization schemes in precipitation prediction is also highlighted in those studies that deal with warm season convective storms (e.g., Fovell 2006; Lowrey and Yang 2008; among others). This study will assess the impact of different WRF parameterization schemes on predicted precipitation, hurricane track, and time of landfall, for Hurricane Rita. This hurricane occurred during September 2005 and was one of the most intense tropical cyclones recorded, causing $11.3 billion in damage along the U.S. Gulf Coast (NHC 2007).

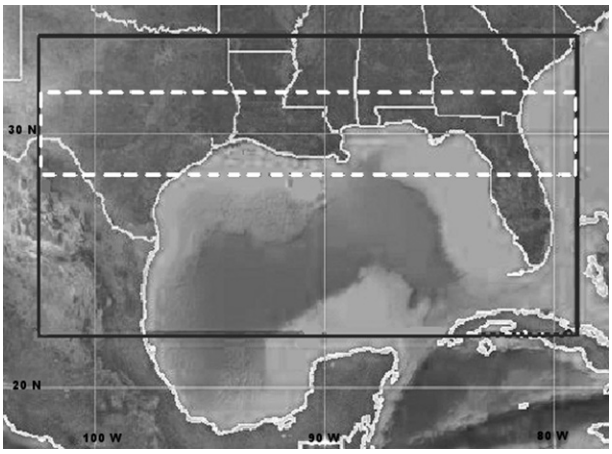

FIG. 1. Model domain used in WRF simulations. The white-dashed rectangular area shows a 2300 km × 400 km area containing 575 × 100 grid cells of 4 km × 4 km where comparisons are made with radar-derived precipitation estimates.

This paper is organized into four sections. In section 2, the model configuration will be briefly introduced. Section 3 will show model results, and the final section of the paper will summarize the conclusions and final remarks.

2. Model configuration and data resources

In this study, WRF version 2.2 was used to simulate Hurricane Rita with a domain consisting of 575 × 320 grid points, 4-km grid size, and 28 vertical levels. The model domain is shown in Fig. 1 (delimited by a black box), and the dashed box in the same figure represents the area used for the model and data comparison (area: 2300 km × 400 km with 575 × 100 grid cells of 4 km). In all simulations, the 6-hourly analyses from the Global Forecast System (GFS), developed by the National Centers for Environmental Prediction (NCEP), were used as the initial and boundary conditions of the model. The simulation was performed in ''predictive'' mode, with observations only updated at boundaries throughout the simulation (i.e., no observation assimilation). The simulation began at 1200 UTC 21 September 2005, and continued until 1200 UTC 25 September 2005. The model settings were based on the Noah land surface model (Chen and Dudhia 2001), the Rapid Radiative Transfer Model (RRTM) longwave radiation scheme (Mlawer et al. 1997), the Dudhia shortwave radiation model (Dudhia 1989), and the Yonsei University (YSU) planetary boundary layer scheme (Hong et al. 2006; Hong and Dudhia 2003).

In this work, various combinations of microphysics schemes and cumulus parameterizations were tested. Five microphysics schemes including Purdue Lin (LIN; Lin et al. 1983), Kessler (KES; Kessler 1969), Ferrier (FER; see Ferrier 1994), Rapid Radiative Transfer Model WSM3 (Hong et al. 2004), and the WRF single-moment five-class microphysics scheme (WSM5; Hong et al. 2004) were utilized. In addition, the following cumulus parameterization schemes were employed: 1) no cumulus parameterization (NCP), 2) Kain–Fritsch (KF; see Kain 2004; Kain and Fritsch 1993; Kain and Fritsch 1990), 3) Betts–Miller–Janjić (BMJ; see Janjić 1994), and 4) Grell–Devenyi (GD; see Grell and Devenyi 2002).

The convective cumulus scheme is mainly used for coarser grid sizes (Skamarock et al. 2007). When the grid size is small enough, one may assume that the convection may be resolved by the grid and, therefore, a cumulus scheme may no longer be needed. Even in finescale simulations, cumulus schemes may be helpful for modeling convective systems and producing realistic rainfall structures (Li and Pu 2009). For example, Li and Pu (2009) demonstrated that using a cumulus scheme at a 9-km grid size improved the simulation results, while the effect of using such parameterization at 3-km grid size had a small impact on the result. Therefore, for a thorough comparison among parameterization schemes, all the cumulus schemes were employed in the simulations. Furthermore, for grid sizes less than 10 km, mixed-phase microphysics schemes (LIN, FER) are recommended for practical applications (Skamarock et al. 2007), as they can account for the interaction of water and ice particles. In this study, other microphysics options were also included in order to verify the necessity of mixed-phase schemes for fine resolutions. The positive-definite transport scheme for moisture was not used in these simulations, even though using this scheme has been shown to reduce the large positive bias in surface precipitation (Skamarock and Weisman 2009).

The 1° GFS data were used in this study as the initial conditions, which will somehow weaken the strength of the hurricane. However, the effect of the initial conditions on the model result is usually quite short, especially for the strong synoptic-scale conditions (Vie et al. 2011). In other words, the use of GFS data as the initial conditions will not significantly affect the landed rainfall caused by the hurricane. It should be mentioned that the modeled rainfall differences (and errors in comparison with reference data) from this study may not only come from the different combinations of microphysics and convective parameterization schemes, but may also come from the nonlinear effects of domain setup and the steep lateral interpolations (downscaling) from 1° GFS data directly onto 4-km WRF grid points. It may also be due to the interactions of the above-mentioned three factors. The effects and interactions are significant especially under strong synoptic-scale circulation conditions like hurricanes (Vie et al. 2011). Using GFS data might also affect the intensity and size of the storm vortex. Previous studies (e.g., Wang et al. 2010) indicate that there is an ''inevitable'' error in simulating hurricane track, whichever lateral boundary schemes are adjusted in the model.

In this study, the reference (i.e., observed) precipitation measurements are based on the stage IV precipitation data (multisensor radar-based gauge-adjusted precipitation data available from NCEP).

3. Results and discussion

a. Precipitation

The stage IV estimates are available at an hourly temporal resolution over the contiguous United States. In this section, the comparisons between the observed and modeled precipitation were performed on hourly and daily bases, as well as throughout the entire period of the model run (4 days). Figure 2 presents the observed and modeled precipitation patterns (in units of mm h^{-1}) using various combinations of cumulus and microphysics schemes at 1000 UTC 24 September 2005. This time step (at 1000 UTC 24 September 2005) is selected as in this time step the entire storm is within the radar coverage. In Fig. 2, each row represents the model results for one microphysical scheme and the different columns show the results of different cumulus parameterizations. Figure 2a displays the stage IV rainfall data in millimeters per hour (i.e., reference dataset). The cumulus scheme represents the subgrid-scale effects of convective and/or shallow clouds due to unresolved updrafts and downdrafts, as shown in Fig. 2, and it has great influence on the distribution of precipitation. It is notable that the KF scheme results in the smallest spatial extent of precipitation, while the LIN–KF simulation exhibits the strongest precipitation over the region. It should be mentioned that although Fig. 2 shows the results for the third day of simulation, some of the models (e.g., WSM3–GD and WSM3–BMJ) can capture the maximum precipitation rate in the northeastern quadrant of the storm.

Table 1 summarizes the results of different model options including the areal extent (km^2), and the average and maximum precipitation (in mm h^{-1}) as an average of 6 h of model results (from 1000 UTC 24 September 2005 until 1600 UTC 24 September 2005).

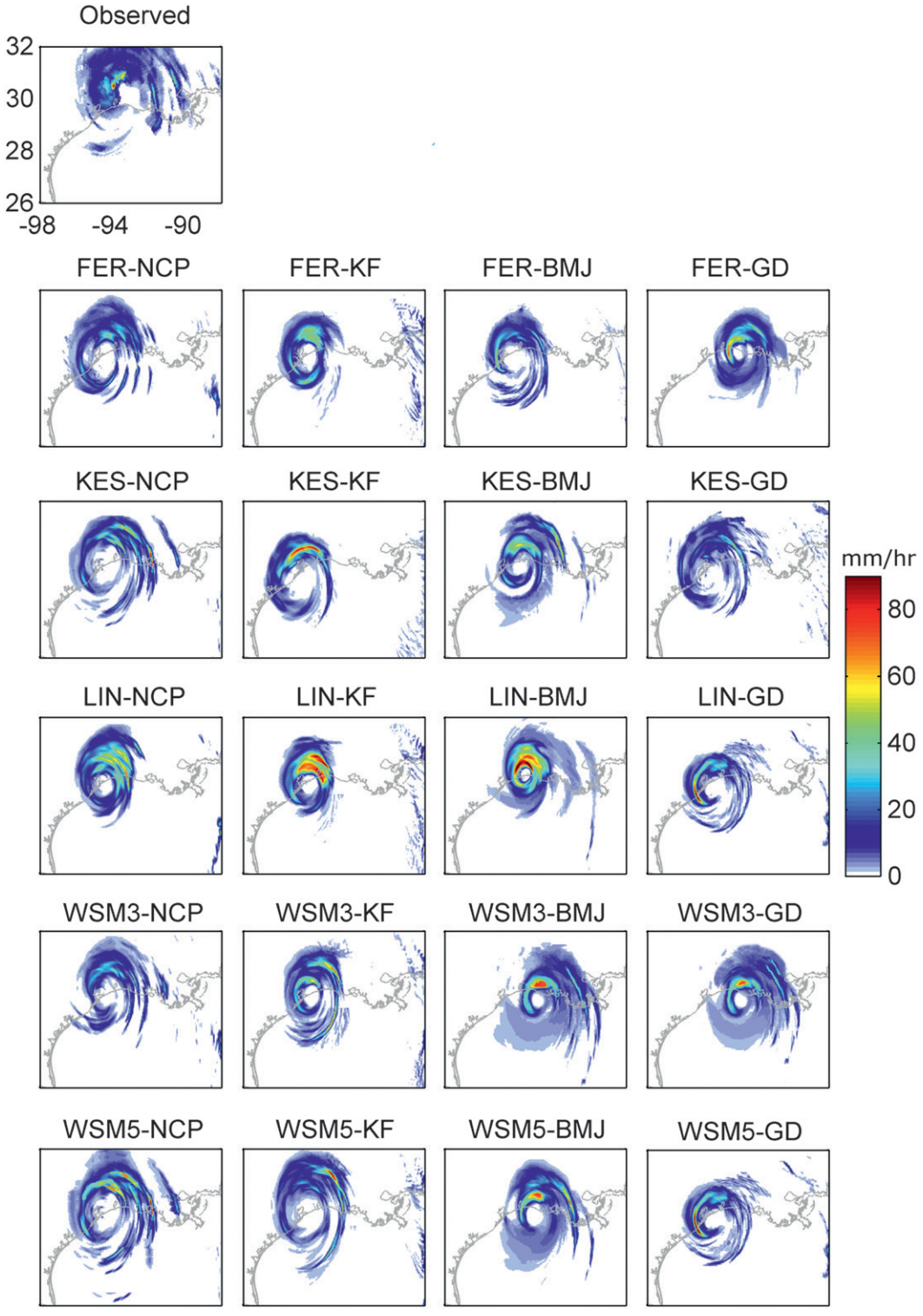

FIG. 2. (top) Observed and (bottom) simulated precipitation patterns (mm h^{-1}) at 1000 UTC on 24 Sep 2005 with different combinations of microphysics and cumulus parameterizations: FER, KES, LIN, WSM3 and WSM5 microphysics; and NCP, KF, BMJ, and GD cumulus parameterizations.

TABLE 1. Averaged values of areal extent, mean, and maximum of observed and simulated precipitation for the time period between 1000 and 1600 UTC 24 Sep 2005 over the selected area shown in Fig. 1.

	Areal extent (km^2)			Mean precipitation ($mm\ h^{-1}$)	Max precipitation ($mm\ h^{-1}$)
	Rainfall threshold ($mm\ h^{-1}$)				
	1	2	10		
FER–NCP	140 504	112 147	31 925	2.6	49.0
FER–KF	92 853	77 747	31 651	2.4	56.7
FER–BMJ	116 037	95 755	23 459	2.1	49.1
FER–GD	124 448	97 949	30 771	2.6	62.8
KES–NCP	152 357	120 301	40 213	3.4	102.0
KES–KF	96 907	78 011	27 939	2.4	76.7
KES–BMJ	128 323	103 101	34 493	2.9	75.3
KES–GD	128 123	102 811	20 696	2.1	69.1
LIN–NCP	121 317	107 373	53 496	4.1	79.8
LIN–KF	94 381	81 725	43 384	4.0	82.6
LIN–BMJ	144 995	114 453	45 021	4.3	118.1
LIN–GD	103 306	82 862	26 654	2.1	64.1
WSM3–NCP	138 061	108 544	29 731	2.4	53.1
WSM3–KF	116 387	96 440	35 037	2.7	74.6
WSM3–BMJ	174 504	140 027	28 413	2.9	69.4
WSM3–GD	177 994	143 527	29 294	2.9	69.4
WSM5–NCP	156 319	123 429	41 259	3.3	101.7
WSM5–KF	137 869	107 933	33 664	2.9	88.5
WSM5–BMJ	139 347	118 245	37 829	3.3	81.6
WSM5–GD	100 688	80 763	25 979	2.1	62.7
Obs	159 467	130 549	40 179	3.6	104.5

It should be noted that the observations are ground-based measurements and do not cover the entire Gulf region. Therefore, a region between 28° and 32°N (within radar coverage) was selected to compare model results with observations. The comparison region is shown with a dashed box in Fig. 1.

The areal extent of the storm was calculated as the number of grid pixels (WRF grid point, hereafter pixel) that exceed a specified rainfall threshold, multiplied by the pixel size. The areas of pixels are calculated using the same map projection for both datasets using ArcGIS. Table 1 lists the areal extents computed based on three thresholds (1, 2, and 10 $mm\ h^{-1}$). Table 2 presents the error (%) of the modeled precipitation with respect to the observations. For rainfall values above all three thresholds, WSM5–NCP and KES–NCP result in the least error in the storm's areal extent. Table 2 also indicates that FER–KF, FER–KF, and KES–GD exhibit the highest error in areal extent simulation for the precipitation thresholds of 1, 2, and 10 $mm\ h^{-1}$, respectively. With respect to the mean and maximum precipitation, KES–NCP is superior to the others.

Figure 3 displays similar comparisons among hourly model results and observations for rainfall values above the 90th percentile, respectively. The 90th percentile was calculated for each simulation with respect to hourly precipitation values above the 1 $mm\ h^{-1}$ threshold (hence different for different simulations). One can see that, for a high threshold (heavy precipitation), the modeled precipitation patterns are very different than the observations. The results indicate that none of the parameterization schemes provide reasonable estimates of extreme patterns and locations. With respect to the magnitudes, while the observation shows precipitation up to ~20 $mm\ h^{-1}$, the LIN scheme predicted higher values, on the order of 50 $mm\ h^{-1}$. Overall, the KES–BMJ scheme was superior with respect to the magnitudes of extremes.

Figure 4 presents the daily average precipitation rates (in $mm\ h^{-1}$) from 0000 to 2400 UTC 24 September 2005. The daily precipitation accumulations clearly highlight the differences between the choices of parameterization schemes. Figure 4 indicates that most parameterization schemes overestimate the amount of rainfall and the extent of high rainfall values (e.g., compare LIN–NCP with observed data). Furthermore, some physics and cumulus options may result in the mislocation of high precipitation values (cf. FER–GD with the observations).

Figure 5 presents the hourly averaged rainfall rates before and after the landfall. This figure shows the hourly averaged precipitation ($mm\ h^{-1}$) area-averaged over the dashed rectangular region that was presented in Fig. 1. The vertical solid line in Fig. 5 represents the time of landfall (0740 UTC 24 September 2005). Figure 5 indicates that the precipitation rates vary significantly

TABLE 2. Error (%) in areal extent, mean, and maximum of simulated precipitation with respect to the observation (averaged results between 1000 and 1600 UTC 24 Sep 2005 over the selected area shown in Fig. 1.

	Areal extent error (%)			Mean precipitation error (%)	Max precipitation error (%)
	Rainfall threshold (mm h^{-1})				
	1	2	10		
FER–NCP	11.89	14.10	20.54	27.72	53.11
FER–KF	41.77	40.45	21.23	34.58	45.77
FER–BMJ	27.23	26.65	41.61	43.06	52.98
FER–GD	21.96	24.97	23.42	27.91	39.87
KES–NCP	4.46	7.85	−0.09	7.64	2.37
KES–KF	39.23	40.24	30.46	33.56	26.65
KES–BMJ	19.53	21.03	14.15	19.77	27.95
KES–GD	19.66	21.25	48.49	41.34	33.90
LIN–NCP	23.92	17.75	−33.15	−14.21	23.69
LIN–KF	40.81	37.40	−7.98	−10.00	20.99
LIN–BMJ	9.08	12.33	−12.05	−19.41	−13.01
LIN–GD	35.22	36.53	33.66	41.38	38.64
WSM3–NCP	13.42	16.86	26.00	33.87	49.16
WSM3–KF	27.02	26.13	12.80	25.62	28.58
WSM3–BMJ	−9.43	−7.26	29.28	19.94	33.56
WSM3–GD	−11.62	−9.94	27.09	19.94	33.56
WSM5–NCP	1.97	5.45	−2.69	7.97	2.66
WSM5–KF	13.54	17.32	16.21	21.03	15.28
WSM5–BMJ	12.62	9.42	5.85	9.88	21.92
WSM5–GD	36.86	38.14	35.34	42.67	40.02

with different model specifications. Figure 5 reveals that the FER and WSM3 microphysics configurations are less variable to the choice of cumulus scheme, while the LIN option shows higher variability of precipitation forecasts with respect to the choice of cumulus parameterizations (cf. Figs. 5a and 5c). Figure 5 also shows that most parameterization options overestimate the amount of precipitation during the last 15 h of simulation. Though the WSM3 scheme both underestimates the total precipitation at the time of landfall and overestimates for the time steps following the landfall, it exhibits better agreement with the observations. It is noted that comparing precipitation amounts for each model run at its respective landfall time would lead to slightly different results (see Table 3 for time of landfall of each simulation and Fig. 5 for hourly rainfall rates).

Figure 6 presents the biases of precipitation accumulations for all 20 combinations of parameterizations before and after the landfall. The top panel in Fig. 6 shows the 24-h bias (prior to landfall) and 12-h bias (after landfall), whereas the bottom panel displays the total bias (96 h: 1200 UTC 21 September–1200 UTC 25 September). Bias is an indication of systematic error, resulting from poor model configuration, model parameterization, deficiencies, parameters, and numerical approximations (Mölders 2008). Another factor that contributes to bias is the fact that a positive-definite transport scheme for moisture was not used in these simulations. It is noted that we have searched extensively for uncertainty estimates in the stage IV precipitation data, and found only limited references to uncertainties in this derived observation product (e.g., Ciach et al. 2007; AghaKouchak et al. 2010b). Since the analysis utilized all available gauge data in conjunction with radar observations, it was difficult to independently estimate uncertainties. In addition, over water there are no rain gauges for bias correction. Therefore, stage IV data over water (near the shoreline) may be biased.

For different combinations of WRF parameterization schemes, the bias values were computed as the ratio of the total predicted to observed rainfall (stage IV precipitation data). A bias of 1.0 indicates the perfect rainfall prediction with respect to the total accumulations, while a bias of more (or less) than 1.0 indicates overestimation (or underestimation) of precipitation accumulations. When calculating the bias value for 25 September, only 12 h of available data were considered. It is worth mentioning that the rainfall accumulations were computed over the comparison region (shown with a dashed box in Fig. 1) where observations are available. Comparing the bias values for 25 September 2005 (after landfall) with 23 September 2005 (before landfall) revealed that the modeled precipitation estimates are more biased over land than over the Gulf (see the top panel in Fig. 6). Comparing all simulations, the WSM3–BMJ and KES–KF combinations resulted in the lowest and highest bias, respectively. It should be noted

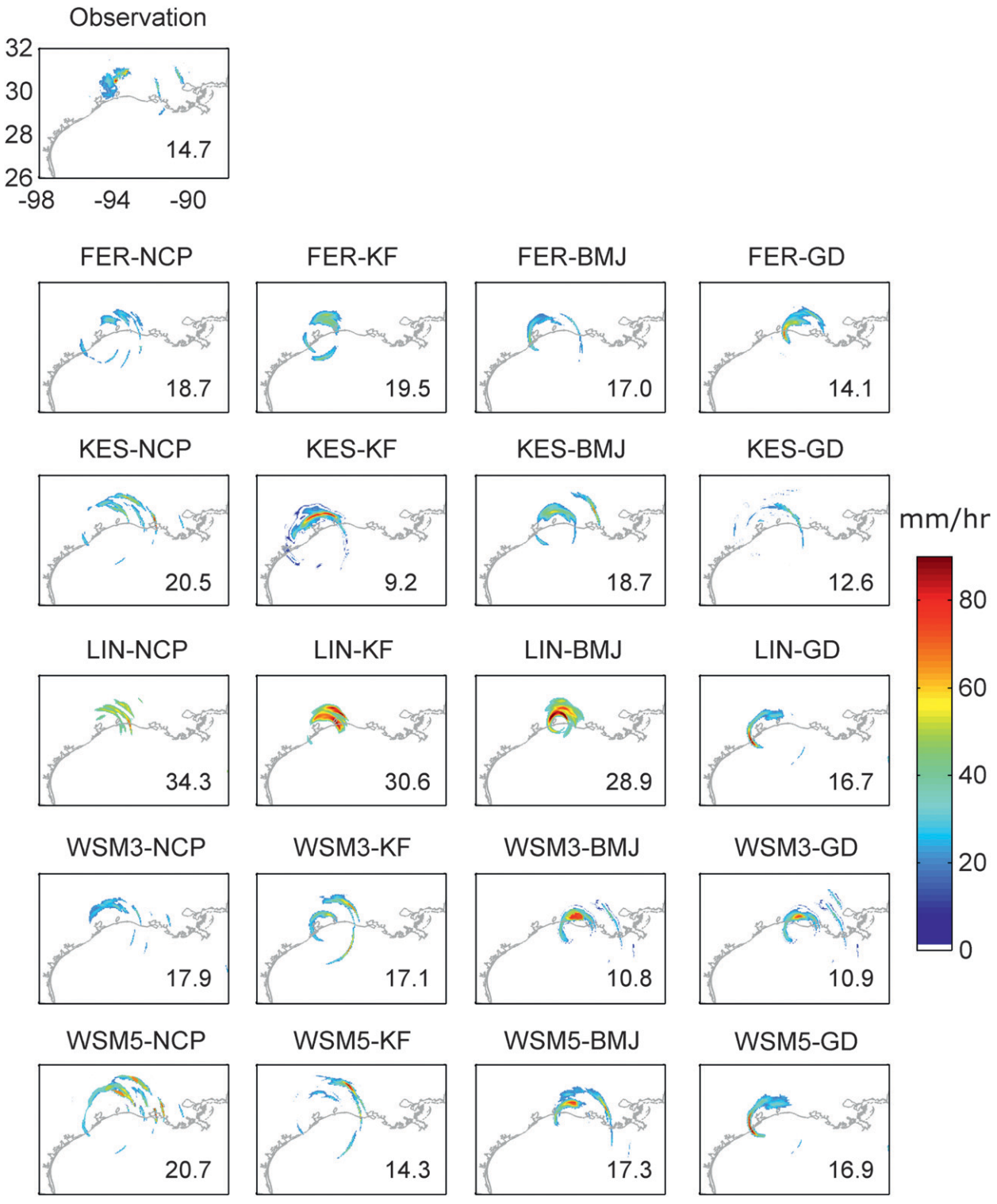

FIG. 3. (top) Observed and (bottom) simulated precipitation patterns (mm h^{-1}) above 90 percentiles at 1000 UTC 24 Sep 2005 (FER, KES, LIN, WSM3, WSM5, NCP, KF, BMJ, and GD). The threshold for each subfigure is shown in mm h^{-1}.

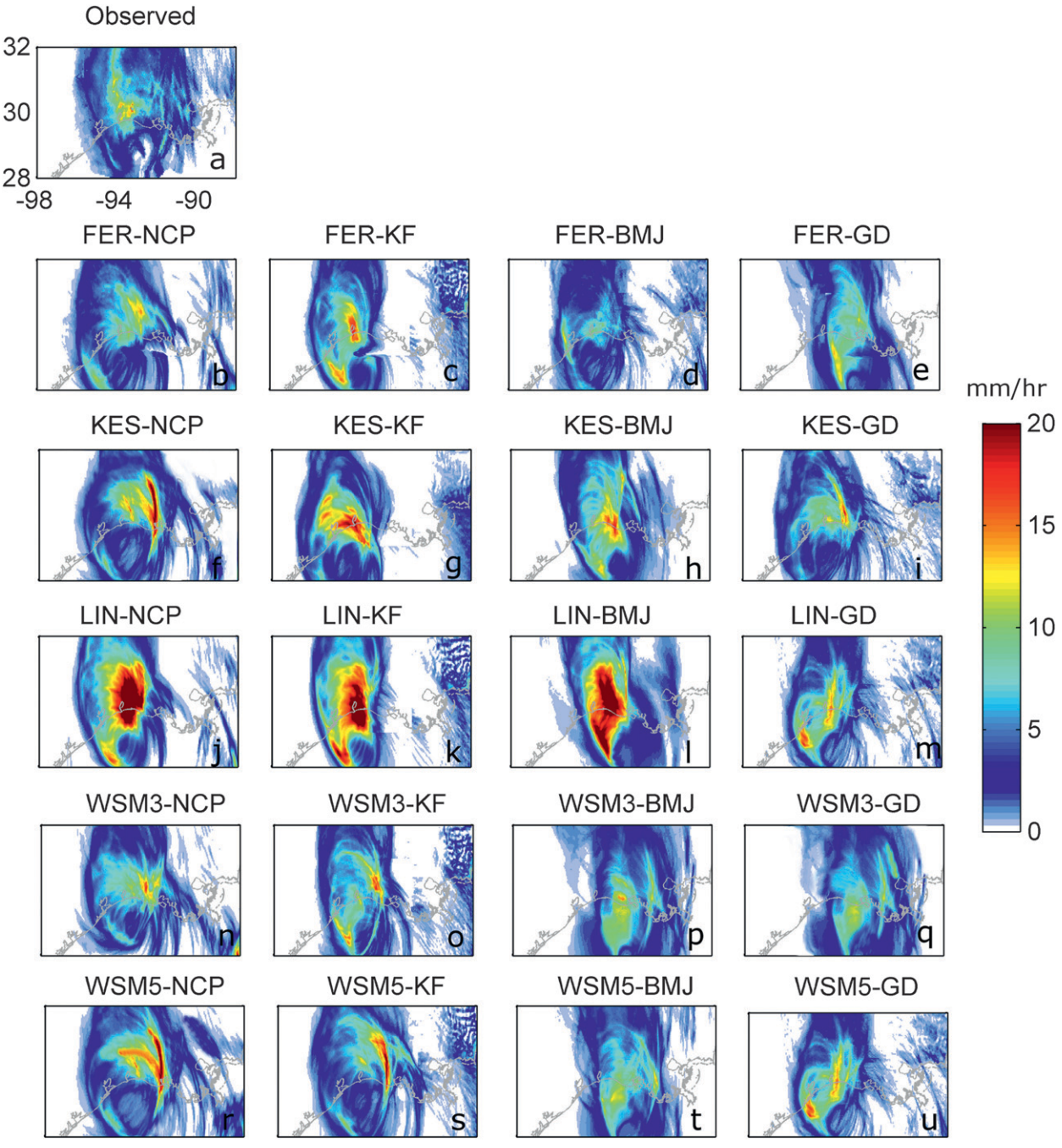

FIG. 4. (top) Observed and (bottom) simulated daily average precipitation rates (mm h^{-1}) from 0000 to 2400 UTC 24 Sep 2005 (FER, KES, LIN, WSM3, WSM5, NCP, KF, BMJ, and GD).

that many of the configurations are within a factor of 2 of the storm total observation, but when smaller time (daily) averages were compared, some configurations fell outside of a factor of 2 of the observations (cf. the top and bottom panels in Fig. 6).

Some combinations of parameterizations exhibit higher variability in bias before and after landfall. For example, simulated rainfall magnitudes with the KES microphysics scheme exhibit bias increases of more than 3 times before and after landfall (see KES–KF, KES–BMJ, and KES–GD in the top panel of Fig. 6). In addition to the daily bias, the total bias was also calculated and is shown in Fig. 6 in the bottom panel for the entire period of the model run (from 1200 UTC 21 September

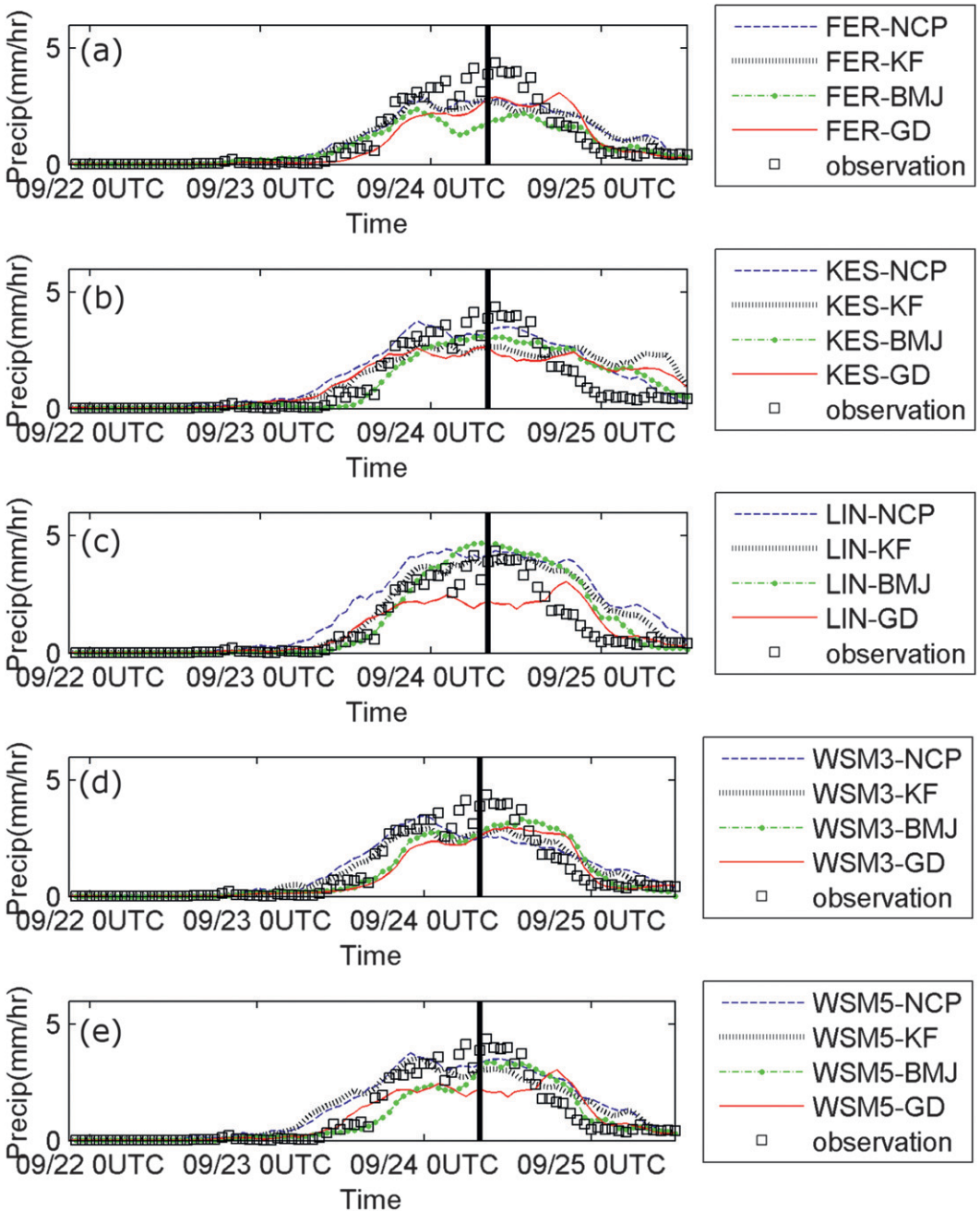

FIG. 5. Hourly averaged rainfall rates spatially averaged over the dashed rectangular region shown in Fig. 1 during 22–25 Sep 2005. Solid black line denotes time of landfall.

to 1200 UTC 25 September). As shown, the overall bias ranges between 0.8 and 1.8 for the FER–BMJ model configuration and LIN–NCP, respectively. Figure 6 indicates that for any given microphysics option, simulations with no convective scheme (–NCP) result in higher bias. Furthermore, for a given microphysics scheme, BMJ and GD exhibit a lesser bias than do NCP and KF. Figure 6 shows that, with respect to the total bias, LIN–GD, WSM5–BMJ, and WSM5–GD lead to a reasonable bias (≈1).

b. *Hurricane track*

Reliable prediction of a hurricane path is of particular importance for decision making and hazard preparedness. Figure 7 displays simulated hurricane tracks using 20 combinations of physics and cumulus options along

TABLE 3. Time of landfall predicted by various parameterization.

Simulation	Time of landfall	Error (h)
FER–NCP	0000 UTC 24 Sep	−8
FER–KF	0400 UTC 24 Sep	−4
FER–BMJ	0500 UTC 24 Sep	−3
FER–GD	0600 UTC 24 Sep	−2
KES–NCP	0100 UTC 24 Sep	−7
KES–KF	0200 UTC 24 Sep	−6
KES–BMJ	0200 UTC 24 Sep	−6
KES–GD	2300 UTC 23 Sep	−9
LIN–NCP	0100 UTC 24 Sep	−7
LIN–KF	0500 UTC 24 Sep	−3
LIN–BMJ	0200 UTC 24 Sep	−6
LIN–GD	0500 UTC 24 Sep	−3
WSM3–NCP	0100 UTC 24 Sep	−7
WSM3–KF	0500 UTC 24 Sep	−3
WSM3–BMJ	0600 UTC 24 Sep	−2
WSM3–GD	0400 UTC 24 Sep	−4
WSM5–NCP	0400 UTC 24 Sep	−4
WSM5–KF	0300 UTC 24 Sep	−5
WSM5–BMJ	0600 UTC 24 Sep	−2
WSM5–GD	0500 UTC 24 Sep	−3

with the actual observed hurricane track (denoted by a solid black line). As shown, the differences between the parameterization schemes become more significant as the hurricane approaches land. When the hurricane is far from land, most parameterization schemes make similar predictions of the hurricane track. However, as the hurricane reaches the land, simulated tracks start to deviate from the observed track. Concurrent with the distance of the hurricane to the land is the run time of the model, which may be another reason for the increased errors near land. The closer to the start of the simulation, the smaller the error is. In should be noted that, when the hurricane reaches the land in the third day of simulation, the errors associated with the length of the model run at that point will also affect the simulated track.

To numerically compare the different parameterization schemes, an average of the track error throughout the 4-day model simulation is computed with respect to the observed track (presented in Fig. 8). As shown, the best storm track forecasts are produced by the BMJ cumulus scheme (LIN–BMJ and KES–BMJ), while the highest mean errors are observed when FER–NCP, WSM3–NCP, and WSM5–NCP were used. In fact, except for when the KES physics option was used, the no-cumulus option (combined with other physics schemes) results in the highest mean error values. Fovell et al. (2010) discussed the sensitivity of hurricane track to the cloud–radiative feedback, which was not activated in these simulations. The cloud–radiative feedback may affect the storm structure, as well as the track of the storm.

c. *Time of landfall*

In addition to the hurricane track, time of landfall was also compared for all combinations of physics and cumulus options. Table 3 lists the time of landfall according to different simulations. The National Hurricane Center (NHC) reported that 0740 UTC 24 September 2005 was the best estimate of the time of landfall. Table 3 indicates that all simulations show earlier landfall compared to observations (values rounded hourly). Among the different combinations, FER–GD, WSM3–BMJ, and WSM5–BMJ predicted the time of landfall most accurately (~2 h earlier). Conversely, FER–NCP and KES–GD provided the least accurate estimates of the time of landfall (~8–9 h earlier).

4. Summary and conclusions

Accuracy and reliability of weather prediction models are vital to our economy and society. Weather prediction models are extensively used for near-real-time forecasting, warning, and decision making. Previous studies showed that microphysics and cumulus schemes are the most sensitive model parameterizations among other physics options for weather prediction models (Fovell 2006; Lowrey and Yang 2008; Jankov et al. 2007; Gallus 1999; Wang and Seaman 1997). This study intends to investigate the performance of the WRF in forecasting precipitation, hurricane track, and time of landfall of Hurricane Rita using different microphysics and cumulus parameterization options. A total of 20 combinations of microphysics and cumulus schemes including five microphysics options and three cumulus parameterizations were investigated, as well as a no-cumulus scheme to validate the WRF outputs against ground-based observations.

While the results showed that model outputs largely depend on the choice of microphysics and cumulus schemes, no single combination can be considered ideal for modeling precipitation amount, areal extent, hurricane track, and the time of landfall. With regard to the precipitation areal extent, the WSM3 and WSM5 physics options were superior to the others, leading to the least error in the precipitation coverage. However, even for various thresholds of precipitation, the best combination of model parameterizations may be different. For example, the results showed that for lower thresholds (1 and 2 mm h^{-1}), the WSM5 option led to the least amount of error in areal extent, whereas given a higher threshold (10 mm h^{-1}), the KES scheme led to the least error. Furthermore, the WSM5–NCP was found to have the best approximation of mean daily precipitation.

The total amounts of daily precipitation values were also compared with observations in order to identify

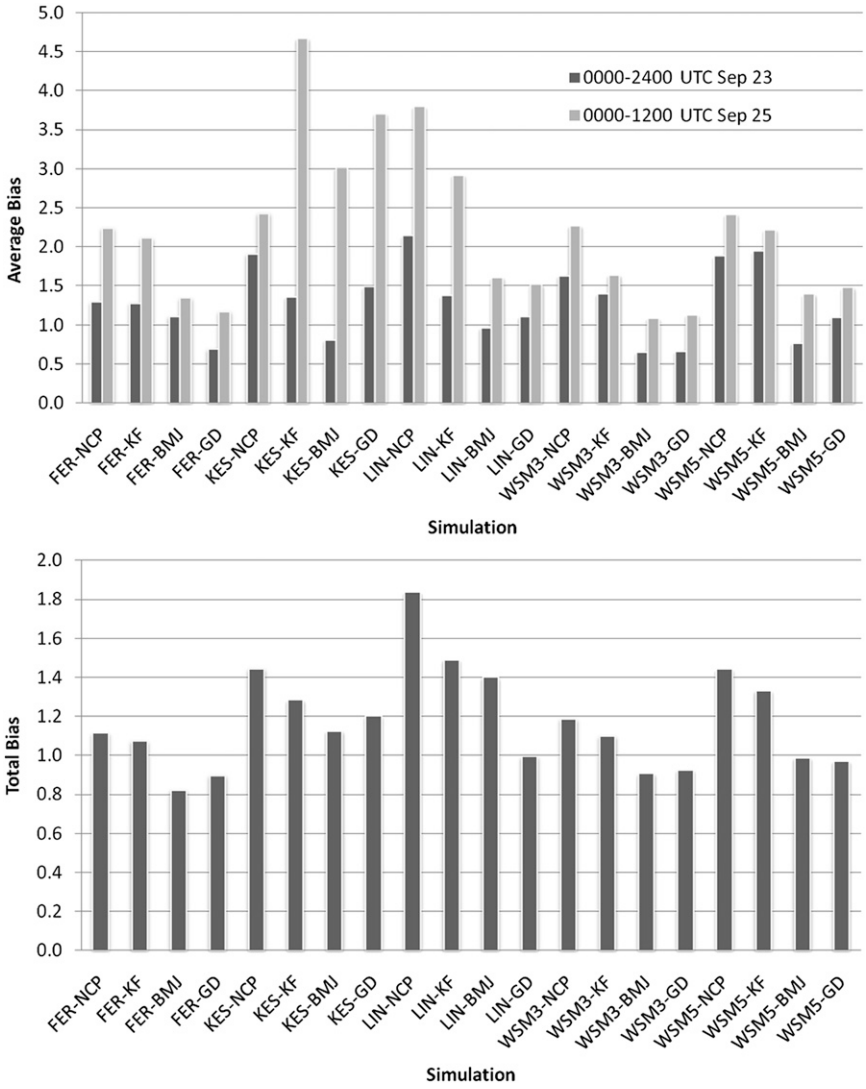

FIG. 6. Average bias in (top) 12-h (0000–1200 UTC 25 Sep) and 24-h (0000–2400 UTC 23 Sep) and (bottom) 96-h (1200 UTC 21 Sep–1200 UTC 25 Sep) precipitation accumulations for different simulations over the dashed rectangular region shown in Fig. 1.

which combination can best simulate cumulative precipitation. The simulated daily precipitation accumulations emphasized the differences between the choices of physics and cumulus schemes. Generally, the simulation scenarios were found to overestimate precipitation accumulation. Furthermore, the results revealed that the overestimations were higher over land than over the Gulf region. Comparing the combinations of parameterizations, WSM3–BMJ led to the best approximation of precipitation over land and over the Gulf region. Furthermore, the results for the BMJ and GD schemes demonstrated lower bias than NCP and KF. Overall, with respect to the precipitation accumulations, LIN–GD, WSM5–BMJ, and WSM5–GD resulted in a more reasonable bias. Moreover, the results showed that simulations with no convective scheme lead to higher bias in precipitation accumulations.

While several combinations of model parameterizations provided reasonable estimates of precipitation, none of the physics and cumulus options provided reliable estimates of heavy precipitation patterns and locations. Object-based pattern analysis methods and geometrical indices can be employed to compare simulated and observed precipitation based on their geometrical characteristics (AghaKouchak et al. 2011). Future developments in model configurations and schemes may be required for capturing precipitation extremes.

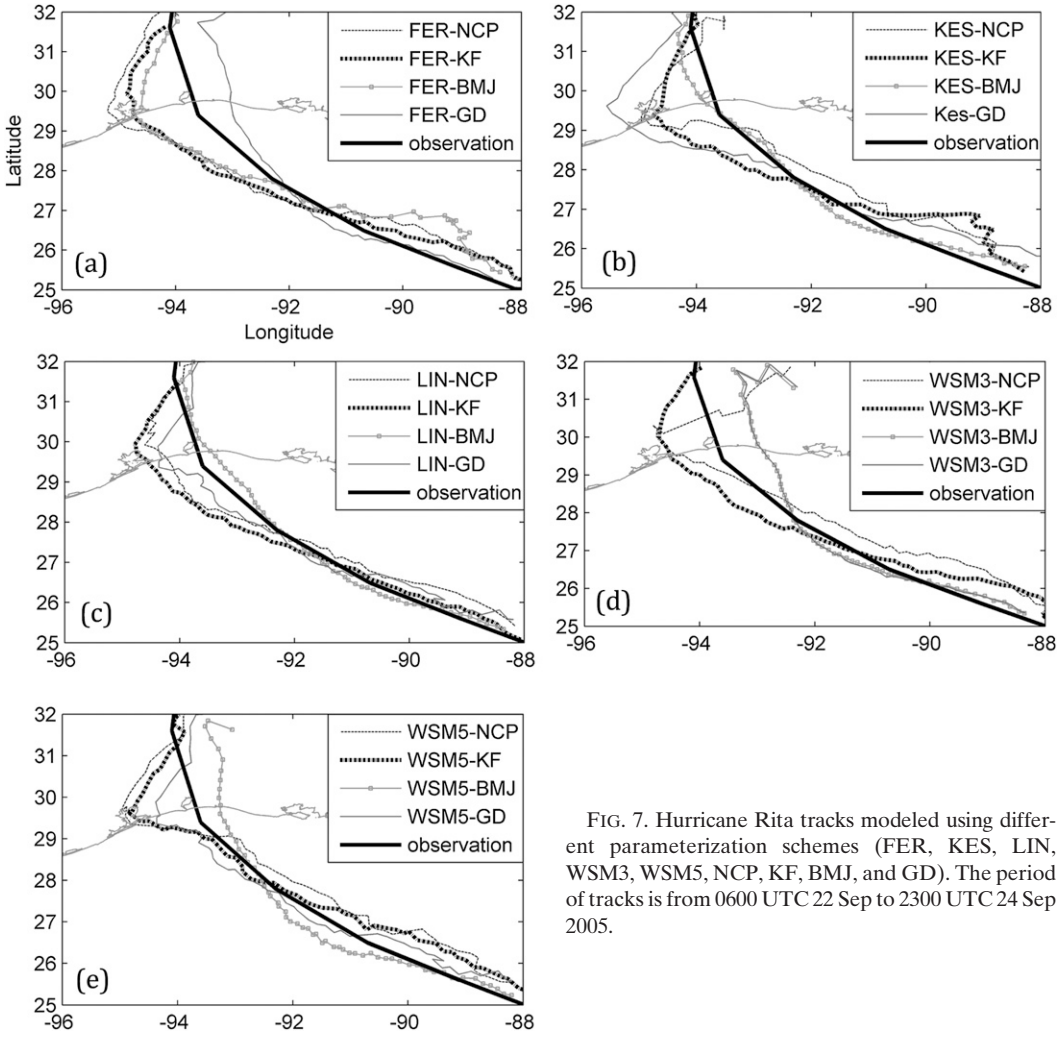

FIG. 7. Hurricane Rita tracks modeled using different parameterization schemes (FER, KES, LIN, WSM3, WSM5, NCP, KF, BMJ, and GD). The period of tracks is from 0600 UTC 22 Sep to 2300 UTC 24 Sep 2005.

In addition to precipitation, the simulated hurricane tracks were compared with the best estimate of the hurricane track obtained from the NHC. The results showed that the model outputs obtained with different parameterization schemes deviated more from each other as simulation time increased and the hurricane approached the land. With respect to the hurricane track, the LIN and KES microphysics options and the BMJ cumulus scheme (LIN–BMJ and KES–BMJ) provided the best hurricane track forecasts.

In summary, the model's ability to generate precipitation was best achieved using the BMJ cumulus parameterization combined with the WSM5 microphysics option. In this case study, WSM5–BMJ simulated the time of landfall with the least error. In predicting the hurricane track, the LIN and KES microphysics and the BMJ cumulus parameterization scheme outperformed other schemes. Some studies have suggested that, for grid sizes smaller than 10 km, using cumulus parameterizations may not be necessary [see Lowrey and Yang (2008) and Skamarock et al. (2007) for a detailed discussion]. However, the results of this study indicate that the use of cumulus schemes improves the model output. This confirms the findings of Lowrey and Yang (2008), which suggest that parameterization of convection AT higher resolutions improves the results.

In addition to the strong sensitivity of WRF to cumulus and physics schemes, accurate forecasting of hurricanes may also rely on other physical options, model processes, and grid resolutions. It should be noted that the results of this study are based on one case study and cannot be generalized for different climate conditions. Future studies using different model configurations for different climate regions are required to validate the results at different climate conditions. Not using the positive-definite transport scheme for moisture may also contribute to

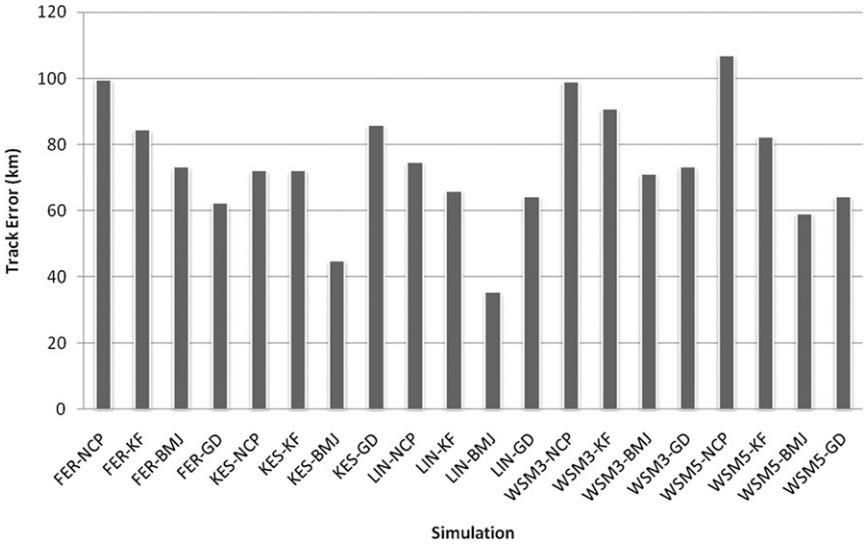

FIG. 8. Hurricane track mean error (km) with respect to the observed path.

large positive bias in surface precipitation. The interaction between simulated cloud and radiation that was not used in this study may affect the track forecast and, hence, other parameters evaluated in the paper.

It is acknowledged that radar-based datasets (e.g., the stage IV data) are subject to various uncertainties. These uncertainties may arise from nonuniformity in the vertical profiles of reflectivity (VPR), anomalous propagation, beam overshooting, partial beam filling, an inappropriate *Z–R* relationship, and spatiotemporal resolution (Seed and Srikanthan 1999; Krajewski and Smith 2002). On the other hand, weather condition can also affect radar-based rainfall estimates (Steiner and Smith 2000). Among the currently available datasets, stage IV estimates are the best area approximation of the true area-average rainfall patterns and values (AghaKouchak et al. 2010a). The stage IV estimates are adjusted for various biases using rain gauge measurements following several quality control measures (Lin and Mitchell 2005). Thus far, numerous studies have attempted to quantify, describe, or adjust for bias in the radar rainfall uncertainties (Seo et al. 1999; AghaKouchak et al. 2010c; Ciach et al. 2007). Generally, quantification of error requires extensive independent ground-based measurements that are not available everywhere, particularly for the stage IV data that already include the NCEP rain gauges in its algorithm. Furthermore, quantification of uncertainties over a certain location (e.g., an experimental watershed) cannot be generalized to different climate regions and conditions. Therefore, no quantitative measure of the uncertainty of the stage IV data is provided. The presented results should be considered as relative comparisons of simulated rainfall fields to the best approximation of observed rainfall.

Acknowledgments. The financial support for this study is made available from NOAA/NESDIS/NCDC (Prime Award NA09NES4400006, NCSU CICS Sub-Award 2009-1380-01), Army Research Office (Award W911NF-11-1-0422), NASA Decision Making Project (Award NNX09AO67G), and NASA Earth and Space Science Fellowship (NNX11AL33H).

REFERENCES

AghaKouchak, A., A. Bárdossy, and E. Habib, 2010a: Conditional simulation of remotely sensed rainfall data using a non-Gaussian v-transformed copula. *Adv. Water Resour.,* **33,** 624–634.

——, ——, and ——, 2010b: Copula-based uncertainty modeling: Application to multi-sensor precipitation estimates. *Hydrol. Processes,* **24,** 2111–2124.

——, E. Habib, and A. Bárdossy, 2010c: Modeling radar rainfall estimation uncertainties: Random error model. *J. Hydrol. Eng.,* **15,** 265–274.

——, N. Nasrollahi, J. Li, B. Imam, and S. Sorooshian, 2011: Geometrical characterization of precipitation patterns. *J. Hydrometeor.,* **12,** 274–285.

Arnaud, P., C. Bouvier, L. Cisner, and R. Dominguez, 2002: Influence of rainfall spatial variability on flood prediction. *J. Hydrol.,* **260,** 216–230.

Chen, F., and J. Dudhia, 2001: Coupling an advanced land surface–hydrology model with the Penn State–NCAR MM5 modeling system. Part I: Model implementation and sensitivity. *Mon. Wea. Rev.,* **129,** 569–585.

Ciach, G., W. Krajewski, and G. Villarini, 2007: Product-error-driven uncertainty model for probabilistic quantitative precipitation estimation with NEXRAD data. *J. Hydrometeor.,* **8,** 1325–1347.

Corradini, C., and V. Singh, 1985: Effect of spatial variability of effective rainfall on direct runoff by geomorphologic approach. *J. Hydrol.,* **81,** 27–43.

Dudhia, J., 1989: Numerical study of convection observed during the Winter Monsoon Experiment using a mesoscale two-dimensional model. *J. Atmos. Sci.,* **46,** 3077–3107.

Ferrier, B. S., 1994: A double-moment multiple-phase four-class bulk ice scheme. Part I: Description. *J. Atmos. Sci.,* **51,** 249–280.

Fiener, P., and K. Auerswald, 2009: Spatial variability of rainfall on a sub-kilometre scale. *Earth Surf. Processes Landforms,* **34,** 848–859.

Fovell, R., 2006: Impact of microphysics on hurricane track and intensity forecasts. *Seventh WRF Users' Workshop,* Boulder, CO, National Center of Atmospheric Research, 3.2. [Available online at http://www.mmm.ucar.edu/wrf/users/workshops/WS2006/abstracts/Session03/3_2_Fovell.pdf.]

——, K. Corbosiero, and H.-C. Kuo, 2010: Influence of cloud-radiative feedback on tropical cyclone motion symmetric contributions. Preprints, *29th Conf. on Hurricanes and Tropical Meteorology,* Tucson, AZ, Amer. Meteor. Soc., 13C.5. [Available online at http://ams.confex.com/ams/pdfpapers/168859.pdf.]

Gallus, W., Jr., 1999: Eta simulations of three extreme rainfall events: Impacts of resolution and choice of convective scheme. *Wea. Forecasting,* **14,** 405–426.

Goodrich, D., J. Faures, D. Woolhiser, L. Lane, and S. Sorooshian, 1995: Measurement and analysis of small-scale convective storm rainfall variability. *J. Hydrol.,* **173,** 283–308.

Grell, G., and D. Devenyi, 2002: A generalized approach to parameterizing convection combining ensemble and data assimilation techniques. *Geophys. Res. Lett.,* **29,** 1693–1696.

Hong, S.-Y., and J. Dudhia, 2003: Testing of a new non-local boundary layer vertical diffusion scheme in numerical weather prediction applications. Preprints, *20th Conf. on Weather Analysis and Forecasting/16th Conf. on Numerical Weather Prediction,* Seattle, WA, Amer. Meteor. Soc., 17.3. [Available online at http://ams.confex.com/ams/pdfpapers/72744.pdf.]

——, ——, and S.-H. Chen, 2004: A revised approach to ice microphysical processes for the bulk parameterization of clouds and precipitation. *Mon. Wea. Rev.,* **132,** 103–120.

Hong, Y., K. Hsu, H. Moradkhani, and S. Sorooshian, 2006: Uncertainty quantification of satellite precipitation estimation and Monte Carlo assessment of the error propagation into hydrologic response. *Water Resour. Res.,* **42,** W08421, doi:10.1029/2005WR004398.

Janjić, Z., 1994: The step-mountain eta coordinate model: Further development of the convection, viscous sublayer, and turbulence closure schemes. *Mon. Wea. Rev.,* **122,** 927–945.

Jankov, I., P. Schultz, C. Anderson, and S. Koch, 2007: The impact of different physical parameterizations and their interactions on cold season QPF in the American River basin. *J. Hydrometeor.,* **8,** 1141–1151.

Kain, J., 2004: The Kain–Fritsch convective parameterization: An update. *J. Appl. Meteor.,* **43,** 170–181.

——, and J. Fritsch, 1990: A one-dimensional entraining/detraining plume model and its application in convective parameterization. *J. Atmos. Sci.,* **47,** 2784–2802.

——, and ——, 1993: Convective parameterization for mesoscale models: The Kain–Fritsch scheme. *The Representation of Cumulus Convection in Numerical Models, Meteor. Monogr.,* No. 46, Amer. Meteor. Soc., 165–170.

Kessler, E., 1969: *On the Distribution and Continuity of Water Substance in Atmospheric Circulation. Meteor. Monogr.,* No. 32, Amer. Meteor. Soc., 84 pp.

Krajewski, W., and J. Smith, 2002: Radar hydrology: Rainfall estimation. *J. Hydrol.,* **25,** 1387–1394.

Li, X., and Z. Pu, 2009: Sensitivity of numerical simulations of the early rapid intensification of Hurricane Emily to cumulus parameterization schemes in different model horizontal resolutions. *J. Meteor. Soc. Japan,* **87,** 403–421.

Lin, Y., and K. Mitchell, 2005: The NCEP stage II/IV hourly precipitation analyses: Development and applications. Preprints, *19th Conf. on Hydrology,* San Diego, CA, Amer. Meteor. Soc., 1.2. [Available online at http://ams.confex.com/ams/pdfpapers/83847.pdf.]

Lin, Y.-L., R. Rarley, and H. Orville, 1983: Bulk parameterization of the snow field in a cloud model. *J. Climate Appl. Meteor.,* **22,** 1065–1092.

Lowrey, M., and Z. Yang, 2008: Assessing the capability of a regional-scale weather model to simulate extreme precipitation patterns and flooding in central Texas. *Wea. Forecasting,* **23,** 1102–1126.

Mlawer, E., S. Taubman, P. Brown, and M. Iacono, 1997: Radiative transfer for inhomogeneous atmospheres: RRTM, a validated correlated-k model for the longwave. *J. Geophys. Res.,* **102** (D14), 16 663–16 682.

Mölders, N., 2008: Suitability of the Weather Research and Forecasting (WRF) model to predict the June 2005 fire weather for interior Alaska. *Wea. Forecasting,* **23,** 953–973.

NHC, 2007: November 2005 Atlantic tropical weather summary. NOAA/National Hurricane Center, 33 pp. [Available online at http://www.nhc.noaa.gov/pdf/TCR-AL182005_Rita.pdf.]

Olson, D. A., N. Junker, and B. Korty, 1995: Evaluation of 33 years of quantitative precipitation forecasting. *Wea. Forecasting,* **10,** 498–511.

Seed, A., and R. Srikanthan, 1999: A space and time model for design storm rainfall. *J. Geophys. Res.,* **104** (D24), 31 623–31 630.

Seo, D.-J., J. Breidenbach, and D. Miller, 1999: Real-time adjustments of mean field and range-dependent biases in WSR-88d rainfall estimation. Preprints, *15th Int. Conf. on Interactive Information and Processing Systems (IIPS) for Meteorology, Oceanography, and Hydrology,* Dallas, TX, Amer. Meteor. Soc., 5.20.

Skamarock, W. C., and M. L. Weisman, 2009: The impact of positive-definite moisture transport on NWP precipitation forecasts. *Mon. Wea. Rev.,* **137,** 488–494.

——, J. Klemp, J. Dudhia, D. Gill, D. Barker, W. Wang, and J. Powers, 2007: A description of the advanced research WRF version 2. NCAR Tech. Note NCAR/TN-468+STR, 88 pp.

Steiner, M., and J. Smith, 2000: Reflectivity, rain rate, and kinetic energy flux relationships based on raindrop spectra. *J. Appl. Meteor.,* **39,** 1923–1940.

Vie, B., O. Nuissier, and V. Ducrocq, 2011: Cloud-resolving ensemble simulations of Mediterranean heavy precipitation events: Uncertainty on initial condition and lateral boundary condition. *Mon. Wea. Rev.,* **139,** 403–419.

Wang, W., and N. Seaman, 1997: A comparison study of convective schemes in a mesoscale model. *Mon. Wea. Rev.,* **125,** 252–278.

Wang, X., Z. Zhong, J. Hu, and H. Yuan, 2010: Effect of lateral boundary scheme on the simulation of tropical cyclone track in regional climate model RegCM3. *Asia-Pac. J. Atmos. Sci.,* **46,** 221–230.

Zhang, F., A. Odins, and J. Nielsen-Gammon, 2006: Mesoscale predictability of an extreme warm-season precipitation event. *Wea. Forecasting,* **21,** 149–166.